

# Order-Disorder and Displacive Behavior of the Cation ( $\text{NH}_4^+$ ) Sites in the Hydrogen-Bonded Antiferroelectric $\text{NH}_4\text{H}_2\text{AsO}_4$ : $^{15}\text{N}$ NMR Evidence

O. GUNAYDIN-SEN, R. FU, R. ACHEY, AND N. S. DALAL\*

Department of Chemistry and Biochemistry and National High Magnetic Field Laboratory, Florida State University, Tallahassee, Florida, 32306, USA

*We report high resolution  $^{15}\text{N}$  NMR measurements of the paraelectric to antiferroelectric phase transition ( $T_N = 216\text{ K}$ ) of the model hydrogen-bonded antiferroelectric  $\text{NH}_4\text{H}_2\text{AsO}_4$  (ADA). We specifically examined whether the  $\text{NH}_4^+$  ions undergo a displacive or an order-disorder behavior at the phase transition. High resolution NMR measurements were made on  $^{15}\text{N}$ -enriched single crystals, using the CPMAS technique at a frequency of 50.6 MHz (11.4T). The temperature dependence of the isotropic chemical shift,  $\delta_{\text{iso}}$ , and of the spin-lattice relaxation time,  $T_1$ , shows clear anomalies at the phase transition. These results are interpreted as evidence for the coexistence of an order-disorder and displacive behavior at the  $\text{NH}_4^+$  site.*

**Keywords**  $^{15}\text{N}$  NMR; hydrogen bonding; antiferroelectric transition; order-disorder phase transition; displacive phase transition

## Introduction

Hydrogen-bonded ferroelectrics and antiferroelectrics of the  $\text{KH}_2\text{PO}_4$  (KDP)-family exhibit structural phase transitions with accompanying anomalous changes in many thermodynamic, dielectric and lattice-dynamical properties [1, 2]. These solids have a very unique property that the hydrogen (H) atoms in the  $\text{O}-\text{H}\cdots\text{O}$  bonds occupy positions in a double-well potential. At temperatures  $T$  above the phase transition, the H's are dynamically disordered within the two sites. Below the transition, the H's localize onto one of the sites, and this results in the onset of a spontaneous polarization [1, 2]. The contribution to the polarization from proton ordering is minor; it arises mainly from the deformation of the rest of the lattice. However, the H's must play a dominant role in the transition mechanism, since isotopic  $\text{H} \rightarrow \text{D}$  substitution leads to a drastic change in the  $T_c$ ; in KDP, for example, the  $T_c$  increases from 123 K to nearly 224 K on deuteration [1]. Blinc, in 1960, was the first to propose that such a large isotope effect must arise from the quantum tunneling of the H atoms in a double potential well [3], but more recent experimental [4–8] and theoretical [9–12] evidence suggests that geometrical effects might be equally, if not more, important, and this is a topic of current research. Another unresolved issue is what roles the other sites

---

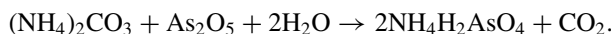
Paper originally presented at IMF-11, Iguassu Falls, Brazil, September 5–9, 2005; received for publication January 26, 2006.

\*Corresponding author. E-mail: dalal@chem.fsu.edu

in the crystal lattice play in the transition mechanism. For example, the substitution of  $\text{NH}_4^+$  in place of  $\text{K}^+$  leads to antiferroelectricity: in going from  $\text{KH}_2\text{AsO}_4$  to  $\text{NH}_4\text{H}_2\text{AsO}_4$  (ADA), the ferroelectric transition at  $T_c = 97$  K changes to an antiferroelectric one at  $T_N = 216$  K [1]. Despite decades of study, however, the origin of this effect is still not clear [13]. One of the issues is whether this cation site is bonded essentially ionically, and undergoes a displacive transition at the  $T_c$ , or does it exhibit an order-disorder character in concert with the protonic motion. Earlier NQR studies by Blinc and coworkers on  $\text{RbH}_2\text{PO}_4$  have suggested a displacive behavior for the Rb sites [14]. EPR studies had indicated that ADA does not exhibit the same behavior as  $\text{KH}_2\text{AsO}_4$ ,  $\text{RbH}_2\text{PO}_4$  and  $\text{CsH}_2\text{AsO}_4$  in terms of  $^{75}\text{As}$  hyperfine splitting,  $A_{\text{iso}}$ , vs. the cation size [15, 16]. Additionally, recent high resolution  $^{31}\text{P}$  NMR studies on  $\text{KD}_2\text{PO}_4$  and  $\text{RbH}_2\text{PO}_4$  have suggested that the  $\text{PO}_4^{3-}$  units exhibit a displacive as well as disorder behavior [17], as reported earlier for squaric acid [18, 19]. In the present work, we have investigated this question for ADA, using the modern high resolution NMR technique of magic angle spinning (MAS) [20]. We measured changes in the isotropic chemical shift,  $\delta_{\text{iso}}$ , of  $^{15}\text{N}$  in the vicinity of the phase transition at 216 K, since it is known that  $\delta_{\text{iso}}$  is a sensitive function of the electronic distribution over the whole molecular unit. The detection of any anomaly in this parameter would be a direct evidence of a change in the electronic structure of the fragment being investigated.  $\delta_{\text{iso}}$  is also invariant to any rotational and translational change of a given molecular unit. We have also measured the temperature dependence of the nuclear spin-lattice relaxation time  $T_1$  for  $^{15}\text{N}$  and compared it with that of the H's and conclude that the  $\text{NH}_4^+$  site exhibits both a displacive and an order-disorder character at the antiferroelectric phase transition.

## Experimental Details

Synthesis and crystal growth: Ammonium Dihydrogen Arsenate (ADA) was prepared by gently evaporating 1:1 mixture of  $\text{As}_2\text{O}_5$  and  $(\text{NH}_4)_2\text{CO}_3$ :



Single crystals were grown by slow evaporation after recrystallization. The crystals had the usual shape like a brick, elongated along the *c*-axis of their tetragonal unit cell.

Labeling:  $^{15}\text{N}$  labeling was obtained by using  $^{15}\text{N}$  enriched  $^{15}\text{NH}_4\text{NO}_3$ . A suitable amount of  $^{15}\text{NH}_4\text{NO}_3$  was added to the ADA solution before the crystallization was started. The  $^{15}\text{N}$  enrichment in the ADA crystals was estimated at  $9 \pm 1\%$ , using NMR.

NMR measurements: A Varian UNITY<sub>INOVA</sub> 500MHz wide-bore solid-state NMR spectrometer was used to measure the CPMAS spectra and  $^{15}\text{N}$  isotropic chemical shifts,  $\delta_{\text{iso}}$  and the relaxation times. The spinning rate was 5 kHz. Signal enhancement was obtained via N—H cross polarization and then proton decoupling during the FID acquisition. The spin-lattice relaxation time  $T_1$  was measured by using the inversion recovery pulse sequence ( $\pi - \tau - \pi/2 \dots$ ), and fitting the FID to Eq. (1) below:

$$M_z(\tau) = M_\infty[1 - 2\exp(-\tau/T_1)] \quad (1)$$

The correlation times,  $\tau_c$ , were obtained from using the Blombergen, Purcell and Pound (BPP) model [21] as discussed below. Temperature variation was obtained by cold  $\text{N}_2$  gas flow, 140 K to 300 K, with closely-spaced (0.2 K) intervals in the close vicinity of the antiferroelectric transition  $T_N = 216$  K.

$^{15}\text{NH}_4^{15}\text{NO}_3$  was used as an internal standard for the  $^{15}\text{N}$  chemical shift variation through the phase transition.

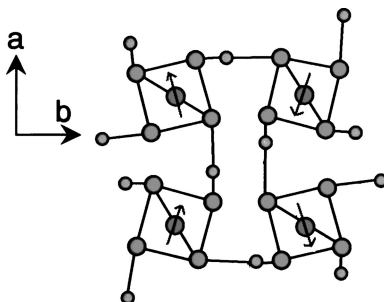


**Figure 1.** *ab* plane projection of the structure of antiferroelectric  $\text{NH}_4\text{H}_2\text{AsO}_4$  (ADA). The arrows point along the dipole moment of an  $\text{H}_2\text{AsO}_4^-$  unit. The dark spheres in the center are As, and the small spheres are the H's in the  $\text{O}-\text{H}\cdots\text{O}$  bonds. (See Color Plate VII)

Structural details: ADA crystallizes in the tetragonal,  $I\bar{4}2d$ , space group at room temperature, and undergoes a phase transition at  $T_N \sim 216$  K to an antiferroelectric phase (orthorhombic  $\text{P}2_12_12_1$ ) [22]. It becomes antiferroelectric, with the H's localized asymmetrically along one of the O's, as shown in Fig. 1.

## Results and Discussion

Figure 2 shows a comparison between  $^{15}\text{N}$  signals from CP-MAS spectra of a crystal of ADA, without any spinning (Fig. 2a) and with spinning at 5 kHz (Fig. 2b). The linewidth decreases from 80 Hz to only about 12 Hz under spinning, demonstrating the significant resolution enhancement provided by the MAS method [20]. The spectrum is a single peak

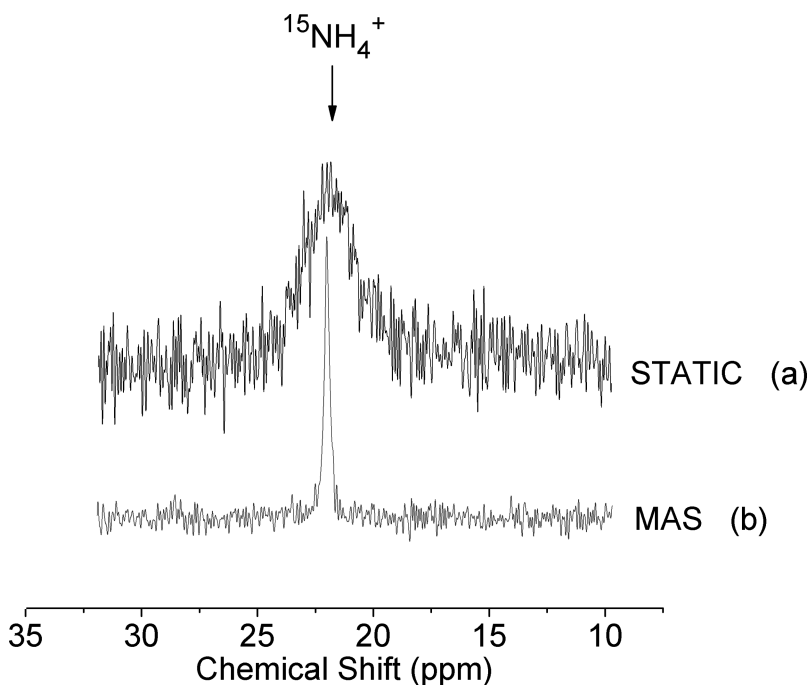


**Figure 2.** Comparison of  $^{15}\text{N}$  NMR spectra for ADA obtained by static (a) and MAS (b) methods.

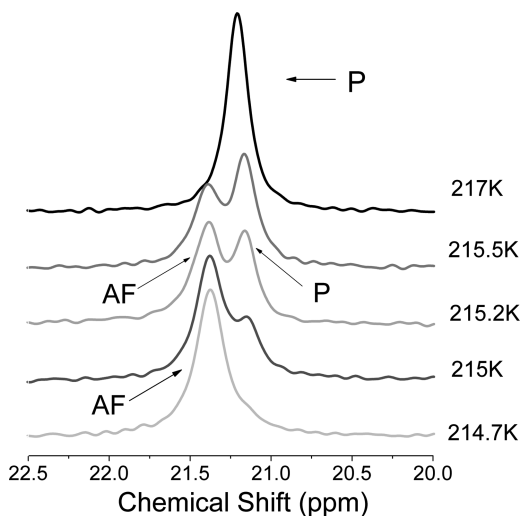


**Figure 3.** Temperature dependence of the  $^{15}\text{N}$  CPMAS spectra around the antiferroelectric phase transition. The peaks corresponding to the paraelectric and antiferroelectric phases are labeled P and AF, respectively. (See Color Plate VIII)

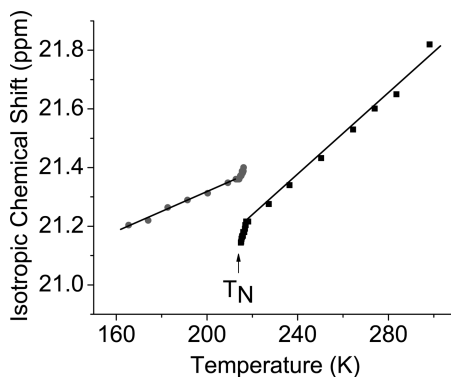
in both the paraelectric ( $T > T_N$ ) and the antiferroelectric ( $T < T_N$ ) phase, centered around 21.3 ppm, which is typical of  $^{15}\text{N}$  from an  $\text{NH}_4^+$  ion [23].

Figure 3 shows the temperature dependence of the  $^{15}\text{N}$  MAS spectra around the transition temperature  $T_N \sim 216$  K.

Figure 4 depicts the temperature dependence of  $\delta_{\text{iso}}$  for  $^{15}\text{N}$  in ADA upon cooling through the  $T_N$ . It is seen that the  $\delta_{\text{iso}}$  for ADA exhibits approximately linear temperature dependence, away from the transition region, both above and below the  $T_N$ .

The temperature dependence of the  $T_1$  for  $^{15}\text{N}$  is shown in Fig. 5. The discontinuity in the  $T_1$  data near  $T_N \sim 216$  K (highlighted by the arrow) appears at the onset of antiferroelectric phase transition. Below  $T_N$ ; the  $T_1$  decreases suddenly from about 700 msec to 370 msec.

We analyzed the temperature dependence of  $T_1$  using the semi-classical, BPP model of the effect of molecular motion on the  $T_1$  [21]. In this model,  $T_1$  can be related to the values



**Figure 4.** Temperature dependence of  $\delta_{\text{iso}}$  of  $^{15}\text{N}$  in ADA. The arrow indicates the antiferroelectric transition temperature,  $T_N$ . A gradual change and then a clear jump marks the phase transition.

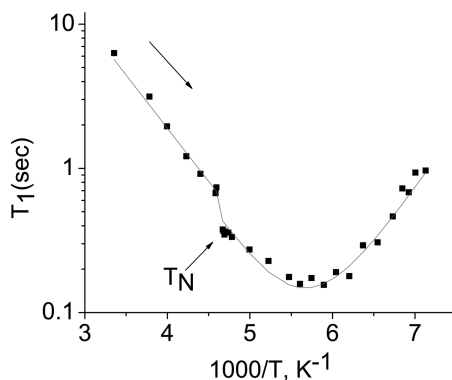


**Figure 5.** Temperature dependence of  $T_1$  for  $^{15}\text{N}$  in ADA at a resonance frequency of 50.7 MHz ( $H_0 = 11.4$  Tesla). Squares are the experimental data points while the curve is the theoretical fit based on Eqs. (1–3) and the parameters presented in Table 1.

of correlation time,  $\tau_c$ , which is the characteristic time between significant fluctuations in the local magnetic field experienced by a spin due to molecular motions or reorientations of a molecule. As usual, it is assumed that  $\tau_c$  follows an Arrhenius like behavior:

$$\tau_c = \tau_0 \exp(E_a/RT) \quad (2)$$

where  $\tau_0$  is the single particle correlation time,  $R$  the gas constant,  $T$  the absolute temperature, and  $E_a$  the activation energy (per mole) for the dynamic process.

The relationship between the spin relaxation rate and the correlation time is expressed by using the BPP equation [21].

$$\frac{1}{T_1} = C \left( \frac{\tau_c}{1 + \omega^2 \tau_c^2} + \frac{4\tau_c}{1 + 4\omega^2 \tau_c^2} \right) \quad (3)$$

where  $\tau_c$  is the correlation time describing the dynamic process,  $\omega$  is the  $^{15}\text{N}$  resonance frequency and  $C$  is the dipole-dipole interaction constant, which is;

$$C = \frac{3}{10} \left( \frac{\mu_0}{4\pi} \frac{\gamma_N \gamma_H \hbar}{r_{\text{NH}}^3} \right)^2 \quad (4)$$

where  $\gamma_N$  and  $\gamma_H$  are the gyromagnetic ratios of  $^{15}\text{N}$  and  $^1\text{H}$ , respectively, and  $r_{\text{NH}}$  is the average N–H bond length. The calculated value for  $C$  was  $1.46 \times 10^9 \text{s}^{-2}$  using the N–H bond length of 1.031 Angstrom taken from  $\text{NH}_4\text{H}_2\text{PO}_4$  [24].

**Table 1**

The Arrhenius parameters for the molecular motion of the  $\text{NH}_4^+$  ion obtained through  $T_1$  measurements at temperatures both above and below  $T_N = 216$  K

Parameter	$T > T_N$	$T < T_N$
$E_a$	$3.4 \pm 0.2$ kcal/mole	$3.5 \pm 0.1$ kcal/mole
$\tau_0$	$7.5 \times 10^{-14}$ s	$9.1 \times 10^{-14}$ s

**Table 2**  
Correlation times for  $^1\text{H}$  and  $^{15}\text{N}$  in  $\text{NH}_4\text{H}_2\text{AsO}_4$

Parameter	250 K	105 K
$^{15}\text{N}, \tau_c$	$7.5 \times 10^{-11}$ s	$2 \times 10^{-8}$ s
$^1\text{H}, \tau_c$ [25]	$3.4 \times 10^{-11}$ s	$1.5 \times 10^{-8}$ s

Figure 5 shows the experimental and calculated temperature dependence of Zeeman spin-lattice relaxation times of nitrogen in ADA. All the experimental data were fitted by using Eqs. (1) and (2), as shown by the solid red lines in Fig. 5, where  $E_a$  and  $\tau_0$  were treated as variables and  $C$  was fixed with using calculated values for N–H bond lengths [24]. The activation energy did not change much from the paraelectric to antiferroelectric phase. The slight increase from 3.4 to 3.5 kcal/mole can be ascribed to increased barrier for ammonium ion reorientations. The activation energies and pre-exponential factors derived from the fitting are given in Table 1.

After fitting the experimental data the correlation times were calculated for the  $^{15}\text{N}$  site. These are tabulated in Table 2. In order to examine the mechanism of the spin-lattice relaxation process, we also determined the  $\tau_c$  for the motion of  $\text{NH}_4^+$  protons using the  $^1\text{H}$   $T_1$  data reported earlier by Grosecu [25] and Dalal et al. [26], using the same procedure as for  $^{15}\text{N}$ . Table 2 shows a comparison of the correlation times between  $^{15}\text{N}$  as measured in the present study and of  $^1\text{H}$  obtained by analyzing the proton  $T_1$  data reported earlier by Grosecu [25]. Close similarity between the two sets of data as seen in Table 2, can be noted implying that the same motion underlies the  $T_1$  process for both nuclei, and relates to the phase transition mechanism. The activation energy ( $E_a$ ) values obtained for the H's were 3.4 and 3.7 kcal/mole for paraelectric and antiferroelectric phases, respectively, which are quite comparable with the corresponding values (3.4 and 3.5 kcal/mol) for  $^{15}\text{N}$ . Note also that the  $\tau_c$  increase by three orders of magnitude in the antiferroelectric phase, showing that the N–H motion slows down anomalously, likely due to the onset of the N–H···O bonding.

## Conclusions

High Resolution  $^{15}\text{N}$  MAS NMR measurements were made on ADA to observe the behavior of the isotropic chemical shift,  $\delta_{\text{iso}}$ , with the temperature in the vicinity of the para-antiferroelectric phase transition at 216 K. The temperature dependence of  $^{15}\text{N}$  isotropic chemical shift,  $\delta_{\text{iso}}$ , showed a clear increase at the antiferroelectric phase transition. The detection of such a change in  $\delta_{\text{iso}}$  is a sensitive function of the total electronic distribution of the whole molecule, and implies that there is a distortion in the molecular structure at the phase transition. This change is evidence of displacive component in the role of  $\text{NH}_4^+$  ion in the phase transition. On the other hand, the motional dynamics observed via the  $T_1$  measurements indicate the presence of the order-disorder behavior at this site.

The temperature dependence of  $T_1$  for ADA also showed clear anomaly at the phase transition showing that the  $\text{NH}_4^+$  motion shows a sudden change at the phase transition. Correlation times and activation energies for the motion of  $^1\text{H}$  and  $^{15}\text{N}$  nuclei are found to be essentially similar indicating that the same motion underlies the  $T_1$  process for both nuclei. The rotational motion of the  $\text{NH}_4^+$  ion slows down by three orders of magnitude, facilitating the N–H···O bond formation, and the onset of the phase transition.

We surmise that the above results would elicit new theoretical and experimental studies on this fascinating system.

## References

1. M. E. Lines and A. M. Glass, Principles and applications of ferroelectrics and related materials. New York: Oxford University Press (2001).
2. R. Blinc and B. Zeks, Soft Modes in Ferroelectrics and Antiferroelectrics. North Holland (1974).
3. R. Blinc, On the isotope effects in the ferroelectric behavior of crystals with short hydrogen bonds. *J. Phys. Chem. Solids* **13**, 204–211 (1960).
4. Z. Tun, R. J. Nelmes, W. F. Kuhs, and R. D. F. Stansfield, A high resolution neutron-diffraction study of the effects of deuteration on the crystal structure of  $\text{KH}_2\text{PO}_4$ . *J. Phys. C: Solid State Phys.* **21**, 245–258 (1988).
5. M. I. McMahon, R. J. Nelmes, W. F. Kuhs, R. Dorwarth, R. O. Piltz, and Z. Tun, Geometric effects of deuteration on hydrogen-ordering phase transitions. *Nature* **348**, 317–319 (1990).
6. J. Seliger and V. Zagar,  $^2\text{H}$  nuclear quadrupole resonance study of the Ubbelohde effect in  $\text{K}(\text{H}_{1-x}\text{D}_x)_2\text{PO}_4$ . *Phys. Rev. B* **59**, 13505–13508 (1999).
7. R. J. Nelmes, M. I. McMahon, R. O. Piltz, and N. G. Wright, High-Pressure neutron-diffraction studies of  $\text{KH}_2\text{PO}_4$ -type phase transition as  $T_C$  tends to 0 K. *Ferroelectrics* **124**, 355–360 (1991).
8. M. Ichikawa, K. Motida, and N. Yamada, Negative evidence for a proton tunneling mechanism in the phase transition. *Phys. Rev. B* **36**, 874–876 (1987).
9. S. Koval, R. L. Kohanoff, R. L. Migoni, and E. Tosatti, Ferroelectricity and isotope effects in hydrogen-bonded KDP crystals. *Phys. Rev. Lett.* **89**, 187602 (2002).
10. S. Koval, J. Kohanoff, J. Lasave, G. Colizzi, and R. L. Migoni, First-principles study of ferroelectricity and isotope effects in H-bonded  $\text{KH}_2\text{PO}_4$  crystals. *Phys. Rev. B* **71**, 184102 (2005).
11. Q. Zhang, F. Chen, N. Kioussis, S. G. Demos, and H. B. Radousky, *Ab initio* study of the electronic and structural properties of the ferroelectric transition in  $\text{KH}_2\text{PO}_4$ . *Phys. Rev. B* **65**, 024108 (2001).
12. J. Lasave, S. Koval, N. S. Dalal, and R. Migoni, Slater and Takagi defects in  $\text{KH}_2\text{PO}_4$  from first principles. *Phys. Rev. B*, **72**, 104104/1–104104/8 (2005).
13. R. Blinc, Order and disorder in ferroelectrics. *Ferroelectrics* **301**, 3–8 (2004).
14. J. Seliger, V. Zagar, and R. Blinc,  $^{85}\text{Rb}$ ,  $^{87}\text{Rb}$ , and  $^{17}\text{O}$  nuclear-quadrupole-resonance study of  $\text{Rb}(\text{H}_{1-x}\text{D}_x)_2\text{PO}_4$ . *Phys. Rev. B* **42**, 3881–3886 (1990).
15. N. S. Dalal, J. R. Dickinson, and C. A. McDowell, Electron Paramagnetic studies of X-irradiated  $\text{KH}_2\text{AsO}_4$ ,  $\text{KD}_2\text{AsO}_4$ ,  $\text{RbH}_2\text{AsO}_4$ ,  $\text{RbD}_2\text{AsO}_4$ ,  $\text{CsH}_2\text{AsO}_4$ ,  $\text{NH}_4\text{H}_2\text{AsO}_4$  and  $\text{ND}_4\text{D}_2\text{AsO}_4$  (Ferroelectrics and Antiferroelectrics). *J. Chem. Phys.* **57**, 4254–4265 (1972). N. S. Dalal, J. A. Hebden, D. E. Kennedy, and C. A. McDowell, EPR and ENDOR study of slow fluctuation and cluster formation in the hydrogen-bonded ferroelectrics  $\text{KH}_2\text{PO}_4$  and  $\text{KD}_2\text{PO}_4$  and antiferroelectrics  $\text{NH}_4\text{H}_2\text{PO}_4$  and  $\text{ND}_4\text{D}_2\text{PO}_4$ . *J. Chem. Phys.* **66**, 4425–4432 (1977).
16. N. S. Dalal, EPR and ENDOR studies of slow dynamics and the central peak phenomenon near phase transitions. *Adv. Mag. Reson.* **10**, 119–215 (1982).
17. A. Bussmann-Holder, N. Dalal, R. Fu, and R. Migoni, High-precision  $^{31}\text{P}$  chemical shift measurements on  $\text{KH}_2\text{PO}_4$ -type crystals: Role of electronic instability in the ferroelectric transition mechanism. *J. Phys.: Condens. Matter* **13**, L231–L237 (2001).
18. N. Dalal, A. Klymchyov, and A. Bussmann-Holder, Coexistence of order-disorder and displacive features at the phase transitions in hydrogen-bonded solids: Squaric acid and its analogs. *Phys. Rev. Lett.* **81**, 5924–5927 (1998).
19. N. S. Dalal, K. L. Pierce, J. Palomar, and R. Fu, Single-crystal magic-angle spinning  $^{17}\text{O}$  NMR and theoretical studies of the antiferroelectric phase transition in squaric acid. *J. Phys. Chem. A* **107**, 3471–3475 (2003).
20. C. A. Fyfe, Solid State NMR for Chemists; CRC Press, Boca Raton, FL (1984).
21. N. Bloembergen, E. M. Purcell, and R. V. Pound, Relaxation effects in nuclear magnetic resonance absorption. *Phys. Rev.* **73**, 679–712 (1947).

22. T. Fukami, X-ray study of crystal structure of  $\text{NH}_4\text{H}_2\text{AsO}_4$  in the paraelectric and antiferroelectric phases. *Phys. Stat. Sol. A* **121**, 383–390 (1990).
23. K. L. Andreson-Altmann and D. M. Grant, A solid-state nitrogen- $^{15}\text{N}$  NMR study of the phase transition in ammonium nitrate. *J. Phys. Chem.* **97**, 11096–11102 (1993).
24. S. Koval, Private communication, in preparation (2005).
25. R. Grosecu, NMR study of molecular reorientations in  $\text{NH}_4\text{H}_2\text{AsO}_4$ . *Chem. Phys. Lett.* **21**, 80 (1973).
26. N. S. Dalal, R. Srinivasan, and C. A. McDowell, Magnetic resonance studies of the antiferroelectric transition in  $\text{NH}_4\text{H}_2\text{AsO}_4$  and  $\text{ND}_4\text{H}_2\text{AsO}_4$ , *J. Chem. Phys.* **60**, 3794–3797 (1974).